# Absorption in flight of positive pions in carbon

D. I. Sober, W. J. Stapor, W. J. Briscoe,* P. E. Burt, Hall Crannell, and J. T. O'Brien†
*Physics Department, The Catholic University of America, Washington D.C. 20064*
(Received 4 June 1979)

We have measured the absorption cross section for positive pions in carbon at four incident energies between 91 and 143 MeV. A detector which was sensitive to the total energy deposited in the target was used to identify pion absorption events. The cross section determined from these measurements rises slowly with increasing energy, supporting some of the recent theoretical predictions in this energy region.

[NUCLEAR REACTIONS $^{12}$C; $\pi^+$ absorption, measured $\sigma(E_\pi)$.]

## I. INTRODUCTION

The importance of true pion absorption in the understanding of meson nuclear physics has been emphasized by many authors.[1-3] True pion absorption (TPA) refers to those processes in which an incident pion interacts with a nucleus and disappears, contributing its rest energy to the kinetic energy of the final state. Because of the requirements of energy-momentum conservation, true absorption cannot occur on a single nucleon. Thus, TPA is an important testing ground for theories of correlations and multistep processes within nuclei. In addition, knowledge of the cross section or mean free path for TPA is a necessary ingredient in the calculation of a wide variety of pion-induced and pion-production reactions. Considering its importance, however, our present knowledge of TPA is very meager.

The pion-nucleus total cross section may be written

$$\sigma_{\rm tot} = \sigma_{\rm el} + \sigma_{\rm inel} + \sigma_{\rm CEX} + \sigma_{\rm abs}\,, \tag{1}$$

where the subscripts on the right side denote elastic scattering, inelastic scattering, charge exchange, and true absorption, respectively. The last three terms comprise the "reaction" cross section. While the pion total, elastic, and reaction cross sections have been satisfactorily measured over a wide energy range for a variety of nuclei,[4,5] the decomposition of the reaction cross section into its inelastic and absorption components has been studied in only a very preliminary and fragmentary fashion. Several previous measurements of the absorption cross section have been performed on carbon[6-12] because of its suitability for a variety of experimental situations. Recently, Navon *et al.*[13] have reported absorption cross sections measured at one energy for a variety of target materials including carbon. These earlier results are summarized in Table I. Both $\pi^+$ and $\pi^-$ cross sections are included in the table, since isospin invariance requires that they be equal for a self-conjugate nucleus. Although there is a rough qualitative consistency among the measured values, it is difficult to generalize about the trend of the absorption cross section with energy because each experiment was performed at a single energy, each data point has its own event selection criteria and experimental biases, and the quoted errors are quite large. Thus, it is not surprising that theoretical calculations of TPA have not been unduly constrained by the available data.

A number of different theoretical approaches have been applied to the calculation of TPA. Sparrow, Sternheim, and Silbar[14,15] used a semiclassical collision model and obtained a phenomenological absorption cross section by fitting to pion-production data. Beder and Bendix[16] used an eikonal model. Werntz and Lucas[17] and, more recently, Stricker, McManus, and Carr[18] and Liu and Shakin[19] have performed calculations in an optical model context. Ginocchio[20] uses an isobar-dominated intranuclear cascade formalism. The results of some of these calculations for carbon, shown in Fig. 1, display a lack of prejudice as to the general trend of the absorption cross section, disagreeing even on whether the cross section is rising or falling as the energy approaches the $\Delta(1232)$ resonance (approximately 150 MeV in carbon). Although the total and elastic cross sections reach their maximum values at the resonance, the increasing opacity of the nucleus tends to reduce the absorption cross section by suppressing the penetration of the pion to the denser nuclear interior, where the probability of interacting with a nucleon pair is greatest. (This phenomenon is illustrated graphically in the paper of Ginocchio.[20]) Thus, all of the theoretical calculations of the TPA cross section are *a priori* plausible. What is required to discriminate between some of the models is a consistent set of measurements of the absorption

 

TABLE I. Previous measurements of the pion absorption cross section in carbon.

| Reference | Pion charge | Detector | Interaction energy ± spread (MeV) | $\sigma_{abs}$ (mb) |
|---|---|---|---|---|
| 8 (Laberrigue, 1959) | + | propane B. C. | 50 ± 20 | 145 ± 36 |
| 11 (Balandin, 1964) | + | propane B. C. | 55 ± 15 | $98^{+17}_{-10}$ |
| | − | propane B. C. | 55 ± 15 | $99^{+24}_{-19}$ |
| 6 (Byfield, 1952) | + | cloud chamber | 62 ± 10 | 153 ± 22 |
| | − | cloud chamber | 62 ± 10 | 148 ± 18 |
| 10 (Salukvadze, 1961) | + | propane B. C. | 78 ± 3 | 180 ± 20 |
| 7 (Kessler, 1954) | − | cloud chamber | 125 ± 10 | 220 ± 40 |
| 12 (Bellotti, 1973) | + | propane B. C. | 133 ± 17 | 189 ± 19 |
| 9 (Petrov, 1959) | + | cloud chamber | 195 ± 15 | 203 ± 22 |
| 13 (Navon, 1979) | + | Scintillation telescope | 125 | 161 ± 28 |
| | − | Scintillation telescope | 125 | 207 ± 30 |

cross section versus pion energy. Our experiment was undertaken in order to provide such data.

## II. EXPERIMENTAL METHOD

Previous experiments have detected outgoing fragments from the absorption events and relied on particle identification and kinematic reconstruction to ascertain that no pion was present in the final state. We have employed a different technique to measure the total cross section for true pion absorption. Our method uses a detector which records the total visible energy associated with each event. In an absorption, the rest energy as well as the kinetic energy of the pion is deposited in the target, whereas in a pion scattering or charge exchange only some fraction of the initial kinetic energy remains in the target.

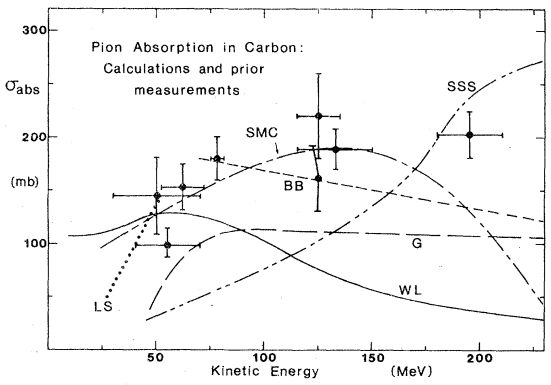


FIG. 1. Results of some theoretical calculations of the pion absorption cross section in carbon. SSS = Sparrow *et al.* (Ref. 14); BB = Beder and Bendix (Ref. 16) (The first two curves have been calculated in Ref. 15, using an effective nucleon number of 7.7); WL = Werntz and Lucas (Ref. 17); SMC = Stricker *et al.* (Ref. 18) (with estimated interpolation between 50 and 180 MeV); LS = Liu and Shakin (Ref. 19); G = Ginocchio (Ref. 20). The data points of Table I are also shown.

In this experiment the carbon target is also the detector. It is composed of 15 plastic scintillation counters (NE102, chemical composition $CH_{1.1}$). The detector target is shown schematically in Fig. 2(a). The main body of the detector consists of a stack of six 0.64-cm thick scintillators labeled $E_1$ through $E_6$ and four 2.5-cm thick scintillators labeled $T_1$ through $T_4$. The beam enters the main stack via a 5-cm diameter hole through two 2.5-cm thick scintillators labeled $H_1$ and $H_2$. A final 0.64-cm thick scintillator labeled $A$ and two scintillators placed along the side labeled $S_1$ and $S_2$ complete the system. An elevation view of the detector system from the perspective of the incident beam direction is shown in Fig. 2(b).

Pions were absorbed in any of the stack ($E$ or $T$) scintillators. The dimensions of the stack were carefully chosen so as to stop nearly all the final-state protons resulting from an absorption for incident pion energies up to 140 MeV. The intranuclear cascade calculations of Bertini[21] were used as a guide to the kinematics in estimating angular distributions of the most energetic protons to be expected from $\pi^+$ incident on carbon

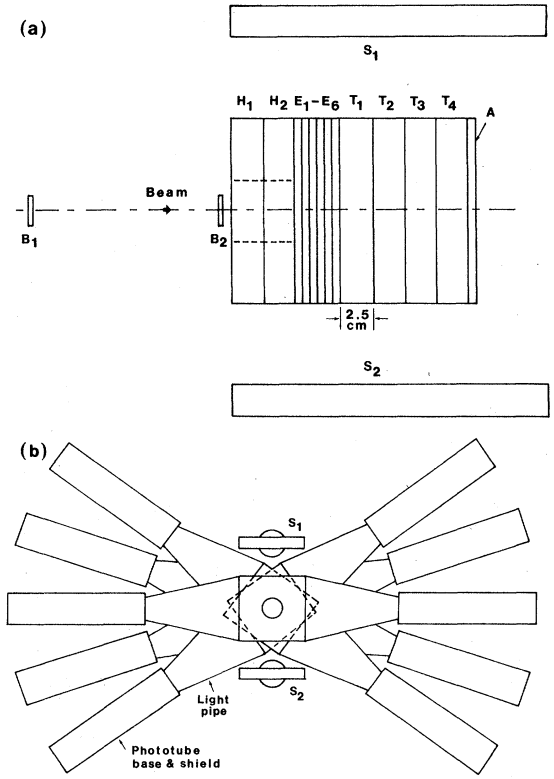


FIG. 2. (a) Configuration of the plastic scintillator array, with light pipes omitted for clarity. The functions of the counters are explained in the text. (b) Schematic view of the apparatus as seen from the incident beam direction.

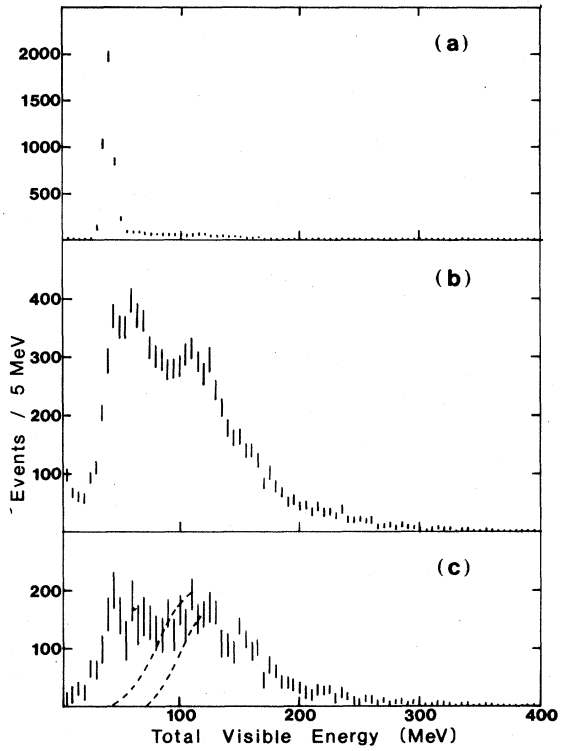


FIG. 3. Total visible energy spectra at 143 MeV for (a) beam run (trigger $B_1B_2$), (b) absorption run (trigger $B_1B_2\bar{A}$), (c) absorption run after side-counter subtraction. The curves in (c) indicate the limits of the various procedures used in excluding events with low visible energy.

at this energy.

In all elastic and almost all inelastic pion scattering events (including scattering from the protons in the plastic), the outgoing pion has enough energy to emerge from the scintillator stack and produce a signal in either the forward anticoincidence counter $A$, a side counter $S_1$-$S_2$, or the backward hole counters $H_1$-$H_2$. The pulse height of this signal in $S_1$, $S_2$, $H_1$, or $H_2$ further identifies the emerging particle as a pion.

The event trigger was provided by a coincidence between two 2.5-cm×2.5-cm beam counters $B_1$ and $B_2$ preceding the array, in anticoincidence with the downstream veto counter $A$ (Fig. 2). Thus, all unscattered or small angle scattered pions were rejected by a signal from $A$. For each event, the pulse height in each of the scintillators, except for $A$, $B_1$, and $B_2$, was recorded. The pulse heights were digitized by a set of LeCroy Model 243 analog-to-digital converters, and the digital outputs were written on magnetic tape by a Digi-Data incremental tape drive, controlled by an interface circuit designed and constructed for this experiment.

Additional "beam" runs were also taken in which the trigger consisted of the coincidence $B_1B_2$ alone. Since the energy lost by pions which traversed the entire detector was known from standard energy-loss tables, these runs allowed for energy calibration of the individual scintillators. A histogram of the total energy deposited in the detector during a beam run, shown in Fig. 3(a), indicates the energy resolution of the system.

Pion beams of kinetic energy 91, 102, 127, and 143 MeV were produced in the meson cave area of the Space Radiation Effects Laboratory in Newport News, Virginia. Beam energy and contamination were determined from range curves taken at each energy. The beam properties are summarized in Table II.

## III. ANALYSIS

The pulse height in each scintillator was converted to a visible energy loss (in MeV) using calibration factors derived from the beam runs.

TABLE II. Properties of incident $\pi$ beams. All tabulated quantities were determined from range curves.

| Nominal energy | 91 MeV | 102 MeV | 127 MeV | 143 MeV |
|---|---|---|---|---|
| Kinetic energy (MeV)[a] | 91.2 ± 1.9 | 102.0 ± 2.2 | 127.2 ± 2.7 | 143.0 ± 3.2 |
| Momentum (MeV/$c$)[a] | 183.8 ± 2.4 | 197.2 ± 2.6 | 227.4 ± 3.2 | 245.7 ± 3.6 |
| Momentum spread[b] | 2.5% | 2.5% | 3.4% | 3.4% |
| Muon fraction | 0.40 ± 0.06 | 0.37 ± 0.05 | 0.29 ± 0.04 | 0.26 ± 0.04 |
| Positron fraction | <0.02 | <0.02 | <0.02 | <0.02 |

[a]Error in central value is due primarily to the ±3% estimated error in degrader thickness.
[b]Standard deviation of distribution, corrected for straggling.

The resulting energy-loss values were then used to construct two types of information: (1) a "total visible energy," equal to the sum of the visible energy losses in the individual counters, and (2) topological information, in particular the identification of outgoing pions in the $S$ and $H$ counters.

Figure 3(b) shows a spectrum of total visible energy for 143-MeV incident pions. A higher-energy peak resulting from pion absorption and a lower-energy peak resulting from large angle elastic and inelastic pion scattering are clearly seen. The number of events in the lower-energy peak is consistent with the known cross sections for pion-proton[22,23] and pion-carbon[5] scattering.

Pions which exit the detector have, for the most part, a reasonably well defined range of energies determined by kinematics and ionization losses in the detector. Those pions which pass through an $S$ or $H$ scintillator are identified by an appropriate small pulse height in this scintillator combined with a low total visible energy in the stack. Less than 3% of the low total visible energy events are anomalous in that they have a large pulse height in a side or hole counter. These anomalous events, which were not used in performing the subtractions discussed below, are probably due to pions which have lost enough energy in inelastic collisions to have a high specific ionization when they reach the side (hole) scintillator and/or to absorption events in which a single proton reaches the side (hole) scintillator with significant energy.

If events with identified outgoing pions are removed from the distribution, one expects only the lower-energy peak to be depleted. Figure 3(c) shows the result of removing such events. (Events with pions in the side counters $S_1$-$S_2$ are subtracted with a weight factor of 3.5, since these counters subtend only 28.6% of the azimuthal angle about the array.) The energy distribution is considerably improved, although there are still low-energy events due to (1) imperfect angular overlap of the $A$ and $S$ detectors allowing escape of some forward scattered pions, (2) escape of some backward scattered pions through the hole in the $H$ detectors, (3) deep inelastic scattering events in which the outgoing pion stops in the array, and (4) charge exchange.

These low-visible-energy events would not be a serious problem except for the fact that some absorption events also have low visible energy because of the presence of energetic nuclear fragments (whose light emission is highly saturated in plastic scintillator) or high-energy neutrons in the final state. Thus, some model is necessary to separate the true absorption from the other remaining contributions. We have used the observations of final-state momentum distributions by Bellotti *et al.*[12] to estimate the minimum visible energy of an absorption event. We take this energy to be that of the least energetic proton from $\pi^+ + d \rightarrow p + p$, corrected for saturation in the scintillator.[24] The resulting minimum visible energy varies between 48 and 58 MeV at our energies. Interpolation between this cutoff and the high-visible-energy peak was performed in a number of ways, with limits indicated by the curves in Fig. 3(c). The error bars on the final results reflect the uncertainties in the cutoff energy and subtraction procedure.

The number of absorption events obtained after these subtractions was between 38 and 44% of the triggers at each energy. Figure 4 indicates the relative sizes of the absorption and nonabsorption contributions to the trigger. The nonabsorption part contains those elastic and inelastic scattering events which were not eliminated by the veto counter. About 65% of these were rejected by the side-counter subtraction, and the remainder by the low-visible-energy cutoff. For comparison, we show the yield calculated from the total cross sections on carbon[5] and hydrogen.[25] The forward veto counter reduces the trigger rate to about 60% of this value.

The effective target thickness used in calculating the cross section is less than the 14.0-cm thickness of the scintillator array because absorption interactions in the last few cm were almost in-

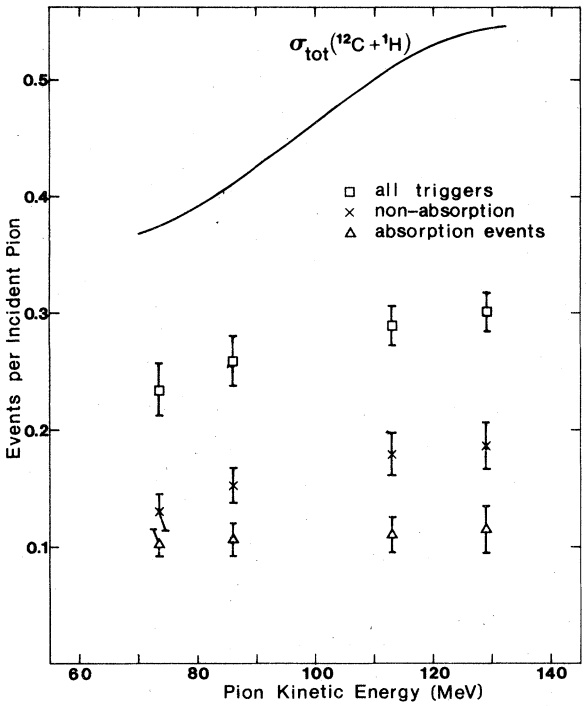


FIG. 4. Yields of events at the four pion energies. The absorption events are selected as described in the text. The solid curve indicates the yield predicted from the sum of the total pion cross sections on carbon (Ref. 5) and hydrogen (Ref. 25).

variably rejected by outgoing charged particles entering the anticoincidence counter. The effective thickness was calculated for each incident energy by reanalyzing the data as a function of target thickness. First $T_4$ and then $T_3$ were treated as the anticoincidence counter, thus simulating the response of stacks with a total thickness of 11.5 and 9.0 cm, respectively. In each case a total visible energy spectrum [as in Fig. 3(b)] was produced. The cross sections for TPA determined from these spectra should be independent of target thickness. The effective thicknesses for these three cases were parametrized as $h$, $h-2.5$, and $h-5.0$ (for total thicknesses 14, 11.5, and 9 cm, respectively) and the value of $h$ was adjusted to minimize $\chi^2$ for deviations of the measured cross sections from a constant value. The effective thickness $h$ of the full 14-cm stack was found to vary from $11.1\pm0.6$ cm at 91 MeV to $9.9\pm0.6$ cm at 143 MeV.

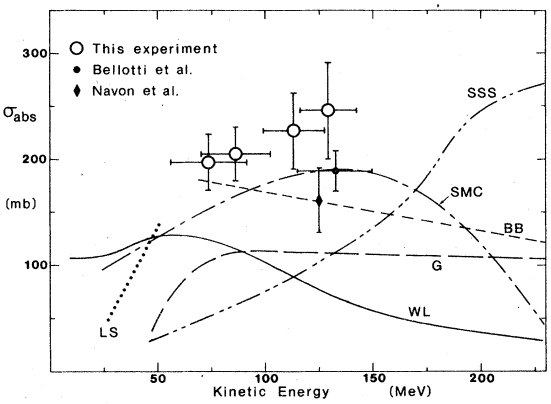


FIG. 5. Absorption cross section measured in this experiment. The horizontal "error bars" indicate the range of interaction energies resulting from energy loss in the target for each incident energy. The data points of Bellotti *et al.* (Ref. 12) and of Navon *et al.* (Ref. 13) are also shown. No horizontal bar is shown for the Navon point because information on the incident kinetic energy spread was not available. The theoretical curves are labeled as in Fig. 1.

## IV. RESULTS AND CONCLUSIONS

The experimental values of the absorption cross section are listed in Table III and plotted in Fig. 5. The error bars include normalization, statistical, and subtraction uncertainties combined in quadrature. The statistical uncertainties alone

TABLE III. Results of this experiment. Errors in the cross section include statistical, normalization, and subtraction errors, which are tabulated separately in columns 3–5.

| Incident energy (MeV) | Interaction energy (MeV) [a] | Experimental uncertainties: Statistical (%) | Normalization (%) [b] | Subtraction (%) | Absorption cross section (mb) |
|---|---|---|---|---|---|
| 91 | 74 ± 17 | 1.6 | 10.9 | 7.3 | 197 ± 26 |
| 102 | 86 ± 16 | 1.6 | 9.8 | 7.3 | 205 ± 25 |
| 127 | 113 ± 14 | 1.7 | 8.1 | 12.9 | 227 ± 35 |
| 143 | 129 ± 14 | 1.8 | 7.9 | 16.7 | 246 ± 46 |

[a] Limits include full range of interaction energies resulting from Coulomb energy loss in the target.

[b] Includes uncertainties in beam and in effective target thickness.

are smaller than the plotted circles. The individual contributions to the uncertainty are given in Table III. A considerable part of the normalization and subtraction uncertainties can be attributed to systematic (i.e., energy-independent) effects. The mean pion interaction energy for each data point is lower than the incident beam energy because of Coulomb energy loss in the target. The horizontal error bars indicate the full range of interaction energies for each point.

The results of this experiment are reasonably consistent with the other data in this energy region. In view of the partial correlation of the uncertainties, our data strongly indicate an absorption cross section which rises with increasing energy. It is interesting to note that the most recent theoretical calculation predicts a gradually rising absorption cross section in this region,[18] in qualitative agreement with the trend and the magnitude of our data. While the general behavior of the absorption cross section with energy seems now to be established, there is certainly a need for more accurate experimental and theoretical work on this problem.

## ACKNOWLEDGMENTS

We gratefully acknowledge the cooperation of Professor Robert Siegel and the (quondam) staff of the Space Radiation Effects Laboratory in the setup and running of this experiment. We thank Professor Carl Werntz for stimulating our interest in this experiment, and for helpful discussions throughout its planning and analysis. This work was supported in part by a Catholic University of America Biomedical Sciences Support Grant, and by National Science Foundation Grant No. PHY 77-26376.

---

*Present address: Department of Physics, University of California, Los Angeles, Calif. 90024.
†Permanent address: Department of Physics and Geoscience, Montgomery College, Rockville, Md. 20850.

[1]J. Hüfner, Phys. Rep. 21C, 1 (1975).
[2]D. S. Koltun, in *Meson-Nuclear Physics–1976, Proceedings of the Carnegie-Mellon Conference*, edited by P. D. Barnes, R. A. Eisenstein, and L. S. Kisslinger (AIP, New York, 1976), p. 1.
[3]F. Lenz, in *Proceedings of the International Conference on High-Energy Physics and Nuclear Structure, Zurich, 1977,* edited by M. P. Locher (Birkhauser, Basel, 1977), Exper. Suppl. 31, p. 175.
[4]V. S. Barashenkov, K. K. Gudima, and V. D. Toneev, Fortschr. Phys. 17, 683 (1969).
[5]F. Binon, P. Duteil, J. P. Garron, J. Gorres, L. Hugon, J. P. Peigneux, C. Schmit, M. Spighel, and J. P. Stroot, Nucl. Phys. B17, 168 (1970).
[6]H. Byfield, J. Kessler, and L. M. Lederman, Phys. Rev. 86, 17 (1952).
[7]J. O. Kessler and L. M. Lederman, Phys. Rev. 94, 689 (1954).
[8]J. V. Laberrigue-Frolova, M. P. Balandin, and S. V. Otvinskii, Zh. Eksp. Teor. Fiz. 37, 634 (1959) [Sov. Phys.-JETP 10, 452 (1960)].
[9]N. I. Petrov, V. G. Ivanov, and V. A. Rusakov, Zh. Eksp. Teor. Fiz. 37, 957 (1959) [Sov. Phys.-JETP 10, 682 (1960)].
[10]R. G. Salukvadze and D. Neagu, Zh. Eksp. Teor. Fiz. 41, 78 (1961) [Sov. Phys.-JETP 14, 59 (1962)].
[11]M. P. Balandin, O. I. Ivanov, V. A. Moiseenko, and G. L. Sokolov, Zh. Eksp. Teor. Fiz. 46, 415 (1964) [Sov. Phys.-JETP 19, 279 (1964)].
[12]E. Bellotti, D. Cavalli, and C. Mateuzzi, Nuovo Cimento 18A, 75 (1973).
[13]I. Navon, D. Ashery, G. Azuelos, H. Pfeiffer, H. Walter, and F. Schlepütz, Phys. Rev. Lett. 42, 1465 (1979).
[14]D. A. Sparrow, M. M. Sternheim, and R. R. Silbar, Phys. Rev. C 10, 2215 (1974).
[15]R. R. Silbar, Phys. Rev. C 11, 1610 (1975).
[16]D. S. Beder, Can. J. Phys. 49, 1211 (1971); D. S. Beder and P. Bendix, Nucl. Phys. B26, 597 (1971).
[17]C. Werntz and C. W. Lucas, *Nuclear Cross Sections and Technology*, edited by R. Schrack and C. D. Bowman (NBS Special Publ. No. 425, Washington D. C., 1975) pp. 472–475; and Report to LASL for Contract NPG-12321-1, Catholic University report, 1976 (unpublished).
[18]K. Stricker, H. McManus, and J. A. Carr, Phys. Rev. C 19, 929 (1979).
[19]L. C. Liu and C. M. Shakin, Phys. Lett. 78B, 389 (1978).
[20]J. N. Ginocchio, Phys. Rev. C 17, 195 (1978).
[21]H. W. Bertini, Phys. Rev. C 6, 631 (1972); Nucl. Phys. 87, 138 (1966); and microfiche output DLC-1 LEP, Oak Ridge National Laboratory (unpublished).
[22]P. J. Bussey, J. R. Carter, D. R. Dance, D. V. Bugg, A. A. Carter, and A. M. Smith, Nucl. Phys. B58, 363 (1973).
[23]J. S. Frank, A. A. Browman, P. A. M. Gram, R. E. Mischke, D. E. Nagle, J. M. Potter, R. P. Redwine, and M. A. Yates-Williams, contribution to the 2nd International Conference on Meson-Nuclear Physics, Houston, Texas, 1979 (unpublished).
[24]T. J. Gooding and H. G. Pugh, Nucl. Instrum. Methods 7, 189 (1960).
[25]A. A. Carter, J. R. Williams, D. V. Bugg, P. J. Bussey, and D. R. Dance, Nucl. Phys. B26, 445 (1971).